Persymmetric Adaptive Radar Detectors

GUILHEM PAILLOUX, Student Member, IEEE
ONERA
France

PHILIPPE FORSTER, Member, IEEE
SATIE
France

JEAN-PHILIPPE OVARLEZ, Member, IEEE
ONERA and SONDRA
France

FRÉDÉRIC PASCAL, Member, IEEE
SONDRA
France

In the general framework of radar detection, estimation of the Gaussian or non-Gaussian clutter covariance matrix is an important point. This matrix commonly exhibits a particular structure: for instance, this is the case for active systems using a symmetrically spaced linear array with constant pulse repetition interval. We propose using the particular persymmetric structure of the covariance matrix to improve the detection performance. In this context, this work provides two new adaptive detectors for Gaussian additive noise and non-Gaussian additive noise which is modeled by the spherically invariant random vector (SIRV). Their statistical properties are then derived and compared with simulations. The vast improvement in their detection performance is demonstrated by way of simulations or experimental ground clutter data. This allows for the analysis of the proposed detectors on both real Gaussian and non-Gaussian data.

I. INTRODUCTION

The problem of adaptive radar detection requires the estimation of the clutter covariance matrix (CCM). In recent years, improvements of the associated estimation schemes have gained tremendous interest in the radar community. For that purpose the sample covariance matrix (SCM) has been widely used and this nonparametric estimator may be improved by exploiting the CCM structure. Toeplitz structure has been addressed by Burg in [1] while Fuhrmann in [2] used this estimator for radar detection purposes. In radar systems using a symmetrically spaced linear array with constant pulse repetition interval, the CCM has the persymmetric property. This structure information could then be exploited to improve detection performance. In this context, we use a particular linear transformation in order to take into account the persymmetry of the CCM and to study the statistical property of new detectors for both Gaussian and non-Gaussian environments. For Gaussian data the CCM maximum likelihood (ML) estimator has been derived in [3]. The corresponding generalized likelihood ratio test (GLRT) has been investigated in [4]. For non-Gaussian clutter modeled by spherically invariant random vectors (SIRVs), detection schemes have been proposed in [5] and [6]. In [5] the persymmetry is only exploited to build two sets of independent data in order to derive a SIRV-constant false alarm rate (CFAR) detector: the persymmetric adaptive normalized matched filter (P-ANMF). In [6] these sets are used to initialize an iterative algorithm simultaneously proposed in [7] and [8]. This allows the derivation of the recursive P-ANMF (RP-ANMF). Our approach, based on the fixed point adaptive normalized matched filter (FP-ANMF), also called GLRT-FP [7, 8], exploits an original transformation already proposed in [9] for Gaussian case and in [10] for non-Gaussian case. This leads to the persymmetric fixed point adaptive normalized matched filter (PFP-ANMF) also called GLRT-PFP, i.e., the persymmetry property of the CCM. Its interest is to render the CCM real, leading to a simpler problem. Moreover this approach allows the derivation of the statistical analysis of the proposed detection scheme.

This paper is organized as follows. Section II presents the studied problem in terms of matrix estimation and radar detection and introduces persymmetry tools where it is shown how the persymmetric structure of the CCM can be exploited to provide the new persymmetric adaptive matched filter (PS-AMF). In Section III we derive the statistical distribution of the PS-AMF under hypothesis H_0, in which only noise is present in order to determine the improvement in terms of probability of false alarm (PFA). To confirm this improvement, some Gaussian data are extracted from the experimental

data to validate the study. Section III also presents similarly the problem in non-Gaussian noise. The purpose is to derive an estimator of the CCM based on the secondary data and to take into account its structure (persymmetric fixed point $\hat{\mathbf{M}}_{\mathrm{PFP}}$). The statistical properties of $\hat{\mathbf{M}}_{\mathrm{PFP}}$ are also established and enable the investigation of the distribution of the detector $\Lambda_{\mathrm{GLRT\text{-}PFP}}$, called GLRT-PFP (generalized likelihood ratio test–persymmetric fixed point). Finally we present in Section IV some simulated and experimental results that illustrate the improvement in terms of detection performance of the PS-AMF with respect to the conventional adaptive matched filter (AMF) for Gaussian case. Moreover, results obtained with non-Gaussian real data demonstrate the interest of the proposed detection scheme compared with the existing detectors P-ANMF, RP-ANMF, and GLRT-FP.

II. BACKGROUND AND PROBLEM STATEMENT

This paragraph provides a guide to the notation used throughout the remainder of the paper. In general, a boldface, lowercase variable indicates a column vector quantity; a boldface, upper variable indicates a matrix; a variable with a caret ($\hat{}$) is an estimate of an unknown quantity. Superscripts $^{\mathrm{T}}$ or $^{\mathrm{H}}$ applied to a vector or a matrix denote the transpose or Hermitian (conjugate) transpose operations. The superscript * denotes the conjugate operation. $E[.]$ stands for the statistical expectation operator, $\mathrm{Tr}(.)$ denotes the trace operator, $\mathrm{Re}(.)$ denotes the real part, and $|.|$ denotes the determinant. In this paper, $\|.\|$ stands for the usual $\mathcal{L}^2$-norm. $\mathbf{I}_m$ is the mth order identity matrix, $\mathrm{Pr}(.)$ stands for the probability, and the notation $\sim$ means "is distributed as."

In radar detection the main problem consists in detecting a signal $A\mathbf{p} \in \mathbb{C}^m$ corrupted by an additive clutter $\mathbf{c}$. This problem can be stated as the following binary hypothesis test:

$$
\begin{aligned}
H_0: \quad & \mathbf{y} = \mathbf{c}, \quad && \mathbf{y}_k = \mathbf{c}_k \quad && \text{for} \quad 1 \le k \le K, \\
H_1: \quad & \mathbf{y} = A\mathbf{p} + \mathbf{c}, \quad && \mathbf{y}_k = \mathbf{c}_k \quad && \text{for} \quad 1 \le k \le K
\end{aligned}
\tag{1}
$$

where $\mathbf{y}$ is the complex m-vector of the received signal, A is an unknown complex target amplitude and $\mathbf{p}$ stands for the known "steering vector." Under both hypotheses, it is assumed that K signal-free data $\mathbf{y}_k$ are available for clutter parameters estimation. The $\mathbf{y}_k$s are the so-called secondary data where they are assumed independent, but their statistical distribution depends on the clutter nature. In this paper two cases are investigated according to the clutter statistics: the Gaussian clutter and the case of non-Gaussian clutter as modeled by SIRV.

A. Gaussian Clutter

In the Gaussian case, $\mathbf{c}$ and $\mathbf{c}_k$ are complex circular zero-mean Gaussian m-vectors sharing the same covariance matrix $\mathbf{M}$, with distribution denoted by $\mathcal{CN}(\mathbf{0}, \mathbf{M})$. When $\mathbf{M}$ is known, the GLRT for A unknown is referred to as the optimum Gaussian detector (OGD):

$$
\Lambda_{\mathrm{OGD}} = \frac{|\mathbf{p}^{\mathrm{H}}\mathbf{M}^{-1}\mathbf{y}|^2}{\mathbf{p}^{\mathrm{H}}\mathbf{M}^{-1}\mathbf{p}} \underset{H_0}{\overset{H_1}{\gtrless}} \lambda_{\mathrm{OGD}}
\tag{2}
$$

where the detection threshold λ_{OGD} is related to the PFA P_{fa} by $\lambda_{\mathrm{OGD}} = -\ln(P_{\mathrm{fa}})$. However, in practice, the CCM $\mathbf{M}$ is generally unknown. One solution is to substitute for $\mathbf{M}$ an estimator $\hat{\mathbf{M}}$ based on the secondary data. When no prior information on the $\mathbf{M}$-structure is available, the SCM is classically used

$$
\hat{\mathbf{M}}_{\mathrm{SCM}} = \frac{1}{K} \sum_{k=1}^{K} \mathbf{y}_k \mathbf{y}_k^{\mathrm{H}}.
\tag{3}
$$

leading to the so-called AMF test [11]:

$$
\Lambda_{\mathrm{AMF}} = \frac{|\mathbf{p}^{\mathrm{H}}\hat{\mathbf{M}}_{\mathrm{SCM}}^{-1}\mathbf{y}|^2}{\mathbf{p}^{\mathrm{H}}\hat{\mathbf{M}}_{\mathrm{SCM}}^{-1}\mathbf{p}} \underset{H_0}{\overset{H_1}{\gtrless}} \lambda_{\mathrm{AMF}}.
\tag{4}
$$

The relationship between the PFA P_{fa} and the detection threshold λ_{AMF} is given by [11, 12]:

$$
P_{\mathrm{fa}} = {}_2F_1\left(K-m+1, K-m+2; K+1; -\frac{\lambda_{\mathrm{AMF}}}{K}\right)
\tag{5}
$$

where ${}_2F_1(.)$ is the hypergeometric function [13] defined by

$$
{}_2F_1(a,b;c;z) = \frac{\Gamma(c)}{\Gamma(b)\Gamma(c-b)} \int_0^1 \frac{t^{b-1}(1-t)^{c-b-1}}{(1-tz)^a} dt.
$$

B. Non-Gaussian Clutter

In recent years, there has been an increasing interest in non-Gaussian clutter models motivated by experimental radar clutter measurements [14], which have shown that the clutter is perfectly modeled by K-distribution or Weibull distribution. More generally, $\mathbf{c}$ can be modeled by a SIRV [15, 16] which is the product of the square root of a positive random variable τ (called the texture) and an m-dimensional independent complex Gaussian vector $\mathbf{g}$ (called the speckle) with zero-mean and covariance matrix $\mathbf{M}$ normalized according to $\mathrm{Tr}(\mathbf{M}) = m$ for identifiability considerations [17]:

$$
\mathbf{c} = \sqrt{\tau}\mathbf{g}.
\tag{6}
$$

The model when $\mathbf{M}$ is known and texture τ is unknown has been widely studied and this enables the construction of the generalized likelihood ratio test–linear quadratic (GLRT-LQ) [18, 17] defined by

$$
\Lambda_{\mathrm{GLRT\text{-}LQ}} = \frac{|\mathbf{p}^{\mathrm{H}}\mathbf{M}^{-1}\mathbf{y}|^2}{(\mathbf{p}^{\mathrm{H}}\mathbf{M}^{-1}\mathbf{p})(\mathbf{y}^{\mathrm{H}}\mathbf{M}^{-1}\mathbf{y})} \underset{H_0}{\overset{H_1}{\gtrless}} \lambda_{\mathrm{GLRT\text{-}LQ}}
\tag{7}
$$

where $\lambda_{\mathrm{GLRT\text{-}LQ}}$ is the corresponding detection threshold.

When $\mathbf{M}$ is unknown, one solution is to substitute a given estimator $\hat{\mathbf{M}}$ of $\mathbf{M}$ in (7) resulting in an adaptive version of the GLRT. When replacing $\mathbf{M}$ by an estimator $\hat{\mathbf{M}}$, this detector is often called adaptive cosine estimate (ACE) [19] or adaptive normalized matched filter (ANMF).

In the non-Gaussian case, the CCM estimator $\hat{\mathbf{M}}$ is based on the signal-free secondary data $\mathbf{y}_k = \mathbf{c}_k$ where the clutter samples $\mathbf{c}_k$ are SIRVs sharing the same CCM as $\mathbf{c}$: $\mathbf{c}_k = \sqrt{\tau_k}\mathbf{g}_k$, where $E[\mathbf{g}_k\mathbf{g}_k^H] = \mathbf{M}$. For the case when no prior information on the $\mathbf{M}$-structure is available, Conte and Gini in [7], [8] proposed an approximate maximum likelihood (AML) estimator $\hat{\mathbf{M}}_{FP}$ of $\mathbf{M}$, called the fixed point (FP) estimator, which is defined as the solution of the following implicit equation:

$$\hat{\mathbf{M}}_{FP} = \frac{m}{K} \sum_{k=1}^{K} \frac{\mathbf{y}_k\mathbf{y}_k^H}{\mathbf{y}_k^H\hat{\mathbf{M}}_{FP}^{-1}\mathbf{y}_k}. \qquad (8)$$

Existence and uniqueness of the above equation solution have been proven in [20], while the complete statistical properties of $\hat{\mathbf{M}}_{FP}$ have been derived in [21]. The estimator $\hat{\mathbf{M}}_{FP}$ does not depend on the texture and allows to obtain the following adaptive detector GLRT-FP:

$$\Lambda_{\text{GLRT-FP}} = \frac{|\mathbf{p}^H\hat{\mathbf{M}}_{FP}^{-1}\mathbf{y}|^2}{(\mathbf{p}^H\hat{\mathbf{M}}_{FP}^{-1}\mathbf{p})(\mathbf{y}^H\hat{\mathbf{M}}_{FP}^{-1}\mathbf{y})} \underset{H_0}{\overset{H_1}{\gtrless}} \lambda_{\text{GLRT-FP}}. \qquad (9)$$

The relationship between the PFA P_{fa} and the detection threshold $\lambda_{\text{GLRT-FP}}$ is given by [22]:

$$P_{fa} = (1 - \lambda_{\text{GLRT-FP}})^{a-1} {}_2F_1(a, a-1; b-1; \lambda_{\text{GLRT-FP}}) \qquad (10)$$

where $K' = (m/(m+1))K$, $a = K' - m + 2$, and $b = K' + 2$.

C. Persymmetry Considerations and Problem Formulation

It is clear that the estimation accuracy of $\hat{\mathbf{M}}$ has an important impact on the adaptive detection performance in both Gaussian and non-Gaussian clutter. $\hat{\mathbf{M}}_{SCM}$ and $\hat{\mathbf{M}}_{FP}$ defined by (3) and (8) do not take into account any prior information on the CCM structure. However many applications lead to a CCM which exhibits some particular structure, and considering this structure may lead to a improvement in both estimation and detection performance. Such a situation is frequently met in radar systems using a symmetrically spaced linear array and a symmetrically spaced pulse train for temporal domain processing [1, 4, 5]. In these systems, the CCM $\mathbf{M}$ has the persymmetric property, defined as follows:

$$\mathbf{M} = \mathbf{J}_m\mathbf{M}^*\mathbf{J}_m \qquad (11)$$

where $\mathbf{J}_m$ is the m-dimensional antidiagonal matrix having 1 as non-zero elements. The steering vector of

the problem is also persymmetric, i.e., it satisfies

$$\mathbf{p} = \mathbf{J}_m\mathbf{p}^*. \qquad (12)$$

The persymmetric structure of $\mathbf{M}$ is exploited in this paper in order to improve its estimation accuracy compared with unstructured estimators. This is done by means of the transformation matrix $\mathbf{T}$ introduced in [23] and whose properties are recalled in the following proposition.

PROPOSITION 1 ([23]) *Let $\mathbf{T}$ be the unitary matrix defined as*

$$\mathbf{T} = \begin{cases} \dfrac{1}{\sqrt{2}} \begin{pmatrix} \mathbf{I}_{m/2} & \mathbf{J}_{m/2} \\ i\mathbf{I}_{m/2} & -i\mathbf{J}_{m/2} \end{pmatrix} & \text{for } m \text{ even} \\[2ex] \dfrac{1}{\sqrt{2}} \begin{pmatrix} \mathbf{I}_{(m-1)/2} & 0 & \mathbf{J}_{(m-1)/2} \\ 0 & \sqrt{2} & 0 \\ i\mathbf{I}_{(m-1)/2} & 0 & -i\mathbf{J}_{(m-1)/2} \end{pmatrix} & \text{for } m \text{ odd.} \end{cases}$$

$$(13)$$

Persymmetric vectors and Hermitian matrices are characterized by the following properties:

1) $\mathbf{p} \in \mathbb{C}^m$ is a persymmetric vector if and only if $\mathbf{Tp}$ is a real vector.

2) $\mathbf{M}$ is a persymmetric Hermitian matrix if and only if $\mathbf{TMT}^H$ is a real symmetric matrix.

Using Proposition 1, the original problem (1) can be equivalently reformulated. Let us introduce the transformed primary data $\mathbf{x}$, the transformed secondary data $\mathbf{x}_k$, the transformed clutter vector $\mathbf{n}$ and the transformed signal steering vector $\mathbf{s}$ defined as: $\mathbf{x} = \mathbf{Ty}$, $\mathbf{x}_k = \mathbf{Ty}_k$, $\mathbf{s} = \mathbf{Tp}$, $\mathbf{n} = \mathbf{Tc}$, $\mathbf{n}_k = \mathbf{Tc}_k$.

It follows that the transformed signal steering vector $\mathbf{s}$ and the transformed CCM are both real. Then, the original problem (1) is equivalent to

$$\begin{array}{llll} H_0: & \mathbf{x} = \mathbf{n} & \mathbf{x}_k = \mathbf{n}_k & \text{for } 1 \le k \le K \\ H_1: & \mathbf{x} = A\mathbf{s} + \mathbf{n} & \mathbf{x}_k = \mathbf{n}_k & \text{for } 1 \le k \le K \end{array} \qquad (14)$$

where $\mathbf{x} \in \mathbb{C}^m$, $\mathbf{s}$ is a known real vector.

In the Gaussian case, under hypothesis H_0, $\mathbf{n}$ and the K transformed secondary data $\mathbf{x}_k$ are independent and identically distributed (IID) and share the same $\mathcal{CN}(\mathbf{0}, \mathbf{R})$ distribution where $\mathbf{R} = \mathbf{TMT}^H$ is a real symmetric matrix according to Proposition 1.

In the non-Gaussian case, one has

$$\mathbf{n} = \sqrt{\tau}\mathbf{h} \qquad (15)$$

$$\mathbf{n}_k = \sqrt{\tau_k}\mathbf{h}_k \qquad (16)$$

where $\mathbf{h} = \mathbf{Tg}$ and $\mathbf{h}_k = \mathbf{Tg}_k$ denote the transformed speckle vector with the same real covariance matrix $\mathbf{R} = \mathbf{TMT}^H$. $\mathbf{n}$ and $\mathbf{n}_k$ are still SIRVs with the same texture and CCM $\mathbf{R} = \mathbf{TMT}^H$. From now on the problem under study is the problem defined by (14).

III. DETECTION SCHEME

In this section the detection problem (14) is investigated in Gaussian and non-Gaussian

frameworks. More precisely, the CCM estimation problem is addressed and adaptive detection schemes are proposed. In both cases, the adaptive detector properties are studied.

A. Detection in Circular Gaussian Noise

Let us first investigate the ML estimator (MLE) of the real covariance matrix $\mathbf{R}$ from the K secondary data $\mathbf{x}_k$. The main motivation for introducing the transformed data is that the resulting distribution of the ML estimator of $\mathbf{R}$ is very simple. This was not the case in [3] when dealing with the original secondary data $\mathbf{y}_k$ with persymmetric covariance matrix.

PROPOSITION 2 *The ML estimator $\hat{\mathbf{R}}_P$ of the real matrix $\mathbf{R}$ is unbiased and is given by*

$$\hat{\mathbf{R}}_P = \mathrm{Re}(\hat{\mathbf{R}}_{\mathrm{SCM}}) \tag{17}$$

where

$$\hat{\mathbf{R}}_{\mathrm{SCM}} = \frac{1}{K}\sum_{k=1}^{K}\mathbf{x}_k\mathbf{x}_k^{\mathrm{H}} = \mathbf{T}\hat{\mathbf{M}}_{\mathrm{SCM}}\mathbf{T}^{\mathrm{H}}. \tag{18}$$

$\hat{\mathbf{R}}_P$ *is an unbiased estimator and $K\hat{\mathbf{R}}_P$ is real Wishart distributed with parameter matrix $\frac{1}{2}\mathbf{R}$ and $2K$ degrees of freedom.*

PROOF It is easy to show that the MLE of the real covariance matrix is provided by (17).

Let us now investigate its statistical properties. Let $\mathbf{a}_k$ and $\mathbf{b}_k$ be the real and imaginary parts of the secondary data:

$$\mathbf{x}_k = \mathbf{a}_k + i\mathbf{b}_k \tag{19}$$

and

$$K\hat{\mathbf{R}}_P = \sum_{k=1}^{K}\mathbf{a}_k\mathbf{a}_k^{\mathrm{T}} + \sum_{k=1}^{K}\mathbf{b}_k\mathbf{b}_k^{\mathrm{T}}. \tag{20}$$

$\mathbf{x}_k$ is circular, i.e., $E[\mathbf{x}_k\mathbf{x}_k^{\mathrm{T}}] = \mathbf{0}$ which leads to

$$\begin{aligned} E[\mathbf{a}_k\mathbf{a}_k^{\mathrm{T}}] - E[\mathbf{b}_k\mathbf{b}_k^{\mathrm{T}}] = \mathbf{0} \\ E[\mathbf{a}_k\mathbf{b}_k^{\mathrm{T}}] + E[\mathbf{b}_k\mathbf{a}_k^{\mathrm{T}}] = \mathbf{0}. \end{aligned} \tag{21}$$

Moreover, $\mathbf{x}_k$ has a real covariance matrix $\mathbf{R}$ which implies:

$$\begin{aligned} E[\mathbf{a}_k\mathbf{a}_k^{\mathrm{T}}] + E[\mathbf{b}_k\mathbf{b}_k^{\mathrm{T}}] = \mathbf{R} \\ E[\mathbf{a}_k\mathbf{b}_k^{\mathrm{T}}] - E[\mathbf{b}_k\mathbf{a}_k^{\mathrm{T}}] = \mathbf{0}. \end{aligned} \tag{22}$$

Equations (21) and (22) yield

$$\begin{aligned} E[\mathbf{a}_k\mathbf{a}_k^{\mathrm{T}}] = E[\mathbf{b}_k\mathbf{b}_k^{\mathrm{T}}] = \tfrac{1}{2}\mathbf{R} \\ E[\mathbf{a}_k\mathbf{b}_k^{\mathrm{T}}] = \mathbf{0} \end{aligned} \tag{23}$$

showing that the $\mathbf{a}_k$s and the $\mathbf{b}_k$s are independent and share the same covariance matrix $\frac{1}{2}\mathbf{R}$.

From (20), $K\hat{\mathbf{R}}_P$ has a real Wishart distribution with $2K$ degrees of freedom and parameter matrix $\frac{1}{2}\mathbf{R}$. Moreover,

$$E[K\hat{\mathbf{R}}_P] = 2K\tfrac{1}{2}\mathbf{R} \tag{24}$$

resulting in $E[\hat{\mathbf{R}}_P] = \mathbf{R}$.

Actually, taking into account the real structure of $\mathbf{R}$ (or equivalently the persymmetric structure of $\mathbf{M}$) in the ML estimation procedure allows to virtually double the number of secondary data. Let us now consider the AMF for the detection problem (14) based on the estimator $\hat{\mathbf{R}}_P$ defined by (17). This leads to the following detection test, called the PS-AMF,

$$\Lambda_{\mathrm{PS\text{-}AMF}} = \frac{|\mathbf{s}^{\mathrm{T}}\hat{\mathbf{R}}_P^{-1}\mathbf{x}|^2}{\mathbf{s}^{\mathrm{T}}\hat{\mathbf{R}}_P^{-1}\mathbf{s}} \underset{H_0}{\overset{H_1}{\gtrless}} \lambda_{\mathrm{PS\text{-}AMF}} \tag{25}$$

or equivalently, in terms of the original data,

$$\Lambda_{\mathrm{PS\text{-}AMF}} = \frac{|\mathbf{p}^{\mathrm{H}}\mathbf{T}^{\mathrm{H}}[\mathrm{Re}(\mathbf{T}\hat{\mathbf{M}}_{\mathrm{SCM}}\mathbf{T}^{\mathrm{H}})]^{-1}\mathbf{T}\mathbf{y}|^2}{\mathbf{p}^{\mathrm{H}}\mathbf{T}^{\mathrm{H}}[\mathrm{Re}(\mathbf{T}\hat{\mathbf{M}}_{\mathrm{SCM}}\mathbf{T}^{\mathrm{H}})]^{-1}\mathbf{T}\mathbf{p}} \underset{H_0}{\overset{H_1}{\gtrless}} \lambda_{\mathrm{PS\text{-}AMF}}. \tag{26}$$

The distribution of (25) is well known when $K\hat{\mathbf{R}}_P$ is complex Wishart distributed with parameter matrix $K\mathbf{R}$ and K degrees of freedom: this is the classical AMF distribution [8, 11]. However, in our problem, $K\hat{\mathbf{R}}_P$ is real Wishart distributed with parameter matrix $\frac{1}{2}\mathbf{R}$ and $2K$ degrees of freedom while $\mathbf{x}$ is complex. The following proposition establishes the statistical distribution of the PS-AMF and the relationship between the PFA P_{fa} and the detection threshold $\lambda_{\mathrm{PS\text{-}AMF}}$.

PROPOSITION 3
1) *Under H_0, the probability density function (pdf) $p(z)$ of $\Lambda_{\mathrm{PS\text{-}AMF}}$, defined by (25), is*

$$\begin{aligned} p(z) = {}&\frac{(2K - m + 1)(2K - m + 2)}{2K(2K + 1)} {}_2F_1 \\ &\times \left(\frac{2K - m + 3}{2}, \frac{2K - m + 4}{2}; \frac{2K + 3}{2}; -\frac{z}{K}\right). \end{aligned} \tag{27}$$

2) *The relationship between P_{fa} and the detection threshold λ is*

$$P_{\mathrm{fa}} = {}_2F_1\left(\frac{2K - m + 1}{2}, \frac{2K - m + 2}{2}; \frac{2K + 1}{2}; -\frac{\lambda_{\mathrm{PS\text{-}AMF}}}{K}\right).$$

PROOF The proof is given in the Appendix, Subsection A.

As seen in Section IV for both simulated and experimental data, the PS-AMF outperforms the AMF, especially for a small number of secondary data.

B. Detection in Non-Gaussian Noise

The purpose of this section is to address the non-Gaussian case for the detection problem (14). Let us first recall some notations. The additive SIRV noise $\mathbf{n}$ is defined by

$$\mathbf{n} = \sqrt{\tau}\mathbf{h} \tag{28}$$

where τ is a positive random variable, and $\mathbf{h}$ is a zero-mean circular complex Gaussian vector with real

CCM $\mathbf{R}$. The K secondary data $\mathbf{n}_k = \sqrt{\tau_k}\mathbf{h}_k$ are IID and share the same distribution as $\mathbf{n}$.

Since the transformed CCM $\mathbf{R}$ is real, its structure may be taken into account in the estimation procedure by retaining only the real part of the FP estimator. This leads to the proposed covariance estimator called the PFP since it results from the persymmetric structure of the original speckle covariance matrix:

$$\hat{\mathbf{R}}_{\mathrm{PFP}} = \mathrm{Re}(\hat{\mathbf{R}}_{\mathrm{FP}}) \qquad (29)$$

with

$$\hat{\mathbf{R}}_{\mathrm{FP}} = \mathbf{T}\hat{\mathbf{M}}_{\mathrm{FP}}\mathbf{T}^{\mathrm{H}}. \qquad (30)$$

In this section, the statistical properties of the detector $\Lambda_{\mathrm{GLRT\text{-}PFP}}$ are investigated under the null hypothesis H_0. Let us recall some basic definitions:

1) A test statistic is said to be texture-CFAR when its distribution is independent of the texture distribution,

2) A test statistic is said to be matrix-CFAR when its distribution is independent of $\mathbf{R}$,

3) A test statistic is said to be SIRV-CFAR when it is both texture-CFAR and matrix-CFAR.

The statistical properties of $\hat{\mathbf{R}}_{\mathrm{PFP}}$ are provided by the following proposition.

PROPOSITION 4 (Statistical Performance of $\hat{\mathbf{R}}_{\mathrm{PFP}}$)

1) *The distribution of $\hat{\mathbf{R}}_{\mathrm{PFP}}$ does not depend on the texture.*

2) $\hat{\mathbf{R}}_{\mathrm{PFP}}$ *is a consistent estimator of* $\mathbf{R}$.

3) $\hat{\mathbf{R}}_{\mathrm{PFP}}$ *is an unbiased estimator of* $\mathbf{R}$.

4) $\hat{\mathbf{R}}_{\mathrm{PFP}}/\mathrm{Tr}(\mathbf{R}^{-1}\hat{\mathbf{R}}_{\mathrm{PFP}})$ *has the same asymptotic distribution as* $\hat{\mathbf{R}}/\mathrm{Tr}(\mathbf{R}^{-1}\hat{\mathbf{R}})$, *where* $\hat{\mathbf{R}}$ *is real Wishart distributed with* $(m/(m+1))2K$ *degrees of freedom and parameter matrix* $\mathbf{R}$.

PROOF   Unbiasedness and consistency of $\hat{\mathbf{R}}_{\mathrm{FP}}$ are proved in [21]. Taking the real part of this estimator does not change these two statistical properties.

It has been shown in [21] that $\hat{\mathbf{R}}_{\mathrm{FP}}/\mathrm{Tr}(\mathbf{R}^{-1}\hat{\mathbf{R}}_{\mathrm{FP}})$ has the same asymptotic distribution as $\hat{\mathbf{R}}_c/\mathrm{Tr}(\mathbf{R}^{-1}\hat{\mathbf{R}}_c)$ with $\hat{\mathbf{R}}_c$ complex Wishart distributed with $(m/(m+1))K$ degrees of freedom and parameter matrix $\mathbf{R}$. Therefore $\hat{\mathbf{R}}_{\mathrm{PFP}}/\mathrm{Tr}(\mathbf{R}^{-1}\hat{\mathbf{R}}_{\mathrm{PFP}})$ has the same asymptotic distribution as $\mathrm{Re}(\hat{\mathbf{R}}_{\mathrm{FP}})/\mathrm{Tr}(\mathbf{R}^{-1}\mathrm{Re}(\hat{\mathbf{R}}_{\mathrm{FP}}))$. By noting that $\mathrm{Tr}(\mathbf{AB}) = \mathrm{Tr}(\mathbf{A}\mathrm{Re}(\mathbf{B}))$ when $\mathbf{A}$ is real symmetric and $\mathbf{B}$ is Hermitian, it follows that $\hat{\mathbf{R}}_{\mathrm{PFP}}/\mathrm{Tr}(\mathbf{R}^{-1}\hat{\mathbf{R}}_{\mathrm{PFP}})$ has the same asymptotic distribution as $\hat{\mathbf{R}}/\mathrm{Tr}(\mathbf{R}^{-1}\hat{\mathbf{R}})$, where $\hat{\mathbf{R}} = 2\mathrm{Re}(\mathbf{R}_c)$ is real Wishart distributed with parameter matrix $\mathbf{R}$ and $K' = (m/(m+1))2K$ degrees of freedom.

DEFINITION 1   The adaptive GLRT, for the transformed problem (14), based on (7) and on the PFP estimator is

$$\Lambda_{\mathrm{GLRT\text{-}PFP}} = \frac{|\mathbf{s}^{\mathrm{T}}\hat{\mathbf{R}}_{\mathrm{PFP}}^{-1}\mathbf{x}|^2}{(\mathbf{s}^{\mathrm{T}}\hat{\mathbf{R}}_{\mathrm{PFP}}^{-1}\mathbf{s})(\mathbf{x}^{\mathrm{H}}\hat{\mathbf{R}}_{\mathrm{PFP}}^{-1}\mathbf{x})} \underset{H_0}{\overset{H_1}{\gtrless}} \lambda_{\mathrm{GLRT\text{-}PFP}}. \quad (31)$$

PROPOSITION 5 $\Lambda_{\mathrm{GLRT\text{-}PFP}}$ *is SIRV-CFAR. For large K, under hypothesis H_0, $\Lambda_{\mathrm{GLRT\text{-}PFP}}$ has the same distribution as* $\Lambda = |\mathbf{e}_1^{\mathrm{T}}\hat{\mathbf{W}}^{-1}\mathbf{w}|^2/(\mathbf{e}_1^{\mathrm{T}}\hat{\mathbf{W}}^{-1}\mathbf{e}_1)(\mathbf{w}^{\mathrm{H}}\hat{\mathbf{W}}^{-1}\mathbf{w})$ *where* $\mathbf{w} \sim \mathcal{CN}(\mathbf{0},\mathbf{I})$, $\mathbf{e}_1 = (1,0,\ldots,0)^{\mathrm{T}}$ *and where $\hat{\mathbf{W}}$ is real Wishart distributed with parameter matrix* $\mathbf{I}$ *and* $K' = (m/(m+1))2K$ *degrees of freedom.*

PROOF   Since the FP estimator $\hat{\mathbf{M}}_{\mathrm{FP}}$ does not depend on the texture, it follows from (29) and (30) that $\hat{\mathbf{R}}_{\mathrm{PFP}}$ is itself texture independent. Moreover, under hypothesis H_0, $\Lambda_{\mathrm{GLRT\text{-}PFP}}$ is homogeneous in terms of τ. Therefore, $\Lambda_{\mathrm{GLRT\text{-}PFP}}$ is texture-CFAR.

Let us now investigate the matrix-CFAR property. Let $\mathbf{R}^{1/2}\mathbf{R}^{\mathrm{T}/2}$ be a real factorization of $\mathbf{R}$, and let $\mathbf{Q}$ be a real unitary matrix such that:

$$\mathbf{Q}\mathbf{R}^{-1/2}\mathbf{s} = (\mathbf{s}^{\mathrm{T}}\mathbf{R}^{-1}\mathbf{s})^{1/2}\mathbf{e}_1. \qquad (32)$$

Note that the last equation is possible with $\mathbf{Q}$ real since $\mathbf{s}$ is itself real. The test statistic $\Lambda_{\mathrm{GLRT\text{-}PFP}}$ may then be rewritten

$$\Lambda_{\mathrm{GLRT\text{-}PFP}} = \frac{|\mathbf{e}_1^{\mathrm{T}}\hat{\mathbf{A}}^{-1}\mathbf{w}|^2}{(\mathbf{e}_1^{\mathrm{T}}\hat{\mathbf{A}}^{-1}\mathbf{e}_1)(\mathbf{w}^{\mathrm{H}}\hat{\mathbf{A}}^{-1}\mathbf{w})} \qquad (33)$$

where

$$\mathbf{w} = \mathbf{Q}\mathbf{R}^{-1/2}\mathbf{h} \sim \mathcal{CN}(\mathbf{0},\mathbf{I}) \qquad (34)$$

and where

$$\hat{\mathbf{A}} = \mathbf{Q}\mathbf{R}^{-1/2}\hat{\mathbf{R}}_{\mathrm{PFP}}\mathbf{R}^{-\mathrm{T}/2}\mathbf{Q}^{\mathrm{T}}$$
$$= \mathrm{Re}(\mathbf{Q}\mathbf{R}^{-1/2}\hat{\mathbf{R}}_{\mathrm{FP}}\mathbf{R}^{-\mathrm{T}/2}\mathbf{Q}^{\mathrm{T}}). \qquad (35)$$

It has been shown in [24] that $\mathbf{Q}\mathbf{R}^{-1/2}\hat{\mathbf{R}}_{\mathrm{FP}}\mathbf{R}^{-\mathrm{T}/2}\mathbf{Q}^{\mathrm{T}}$ in (35) is an FP estimator of the identity matrix and that its distribution is therefore independent of $\mathbf{R}$. Thus, the same conclusion holds for its real part $\hat{\mathbf{A}}$ defined by (35) and the matrix-CFAR property is proved.

From the fourth point of Proposition 4, $\Lambda_{\mathrm{GLRT\text{-}PFP}}$ has the same distribution as

$$\Lambda = \frac{|\mathbf{s}^{\mathrm{T}}\hat{\mathbf{R}}^{-1}\mathbf{x}|^2}{(\mathbf{s}^{\mathrm{T}}\hat{\mathbf{R}}^{-1}\mathbf{s})(\mathbf{x}^{\mathrm{H}}\hat{\mathbf{R}}^{-1}\mathbf{x})} \qquad (36)$$

where $\hat{\mathbf{R}}$ is real Wishart distributed with K' degrees of freedom and parameter matrix $\mathbf{R}$.

Let $\mathbf{Q}$ be the real unitary matrix defined by (32) and let us define $\hat{\mathbf{W}} = \mathbf{Q}\mathbf{R}^{-1/2}\hat{\mathbf{R}}\mathbf{R}^{-\mathrm{T}/2}\mathbf{Q}^{\mathrm{T}}$. The matrix $\hat{\mathbf{W}}$ is real Wishart distributed with K' degrees of freedom and parameter matrix $\mathbf{I}$. Then Λ defined by (36) can be rewritten as

$$\Lambda = \frac{|\mathbf{e}_1^{\mathrm{T}}\hat{\mathbf{W}}^{-1}\mathbf{w}|^2}{(\mathbf{e}_1^{\mathrm{T}}\hat{\mathbf{W}}^{-1}\mathbf{e}_1)(\mathbf{w}^{\mathrm{H}}\hat{\mathbf{W}}^{-1}\mathbf{w})} \qquad (37)$$

which concludes the proof.

Moreover, in the sequel, all the statistical properties can be analyzed by choosing $\mathbf{n}$ and $\mathbf{n}_k$ to be Gaussian distributed because of these texture-CFAR properties. The analytical expression for the pdf of

the detector $\Lambda_{\text{GLRT-PFP}}$ has not been derived but the following proposition gives some insight about its distribution. This derivation is important from an operational point of view in order to regulate the false alarm.

PROPOSITION 6   *For large K, $\Lambda_{\text{GLRT-PFP}}$ has the same distribution as $F/(F + 1)$ where*

$$F = \frac{(\alpha_1 l_{22} - \alpha_2 l_{21})^2 + \left(1 + \left(\frac{\beta_3}{l_{33}}\right)^2\right)(al_{22} - bl_{21})^2}{(\alpha_2 l_{11})^2 + \left(l_{11} l_{22} \frac{\beta_3}{l_{33}}\right)^2 + l_{11}^2 \left(1 + \left(\frac{\beta_3}{l_{33}}\right)^2\right)b^2} \tag{38}$$

and where all the following random variables are independent and distributed according to

$$a, b, \alpha_1, l_{21} \sim \mathcal{N}(0,1), \qquad \alpha_2^2 \sim \chi_{m-1}^2, \qquad \beta_3^2 \sim \chi_{m-2}^2$$

$$l_{11}^2 \sim \chi_{K'-m+1}^2, \qquad l_{22}^2 \sim \chi_{K'-m+2}^2, \qquad l_{33}^2 \sim \chi_{K'-m+3}^2$$

with $K' = (m/(m + 1))2K$.

PROOF   The proof of this proposition is given in the Appendix, Subsection B.

Proposition 6 may be used to obtain, through Monte-Carlo simulations, the relation between the PFA and the detection threshold λ for the GRLT-PFP (31).

IV.   VALIDATION ON EXPERIMENTAL DATA

After the statistical study of these detectors, this section presents some results obtained on some experimental and simulated data in Gaussian and non-Gaussian cases.

A.   Experimental Gaussian Data Extraction and Validation

The ground clutter data used in this paper were collected by an operational radar at Thales Air System. The radar is 13 m above the ground and illuminating the ground at low grazing angle. Ground clutter complex echoes were collected for $N = 868$ range bins, for 70 different azimuth angles, and for $m = 8$ pulses. Fig. 1 displays the ground clutter data level (in dB) corresponding to the first pulse echo. Near the radar, echoes characterize heterogeneous ground clutter whereas beyond the radioelectric horizon of the radar (around 15 km), only heterogeneous thermal noise (the blue part of the map) is present.

In order to test the PS-AMF and given the non-Gaussian nature of experimental data, it is necessary to select particular data on the radar map. In addition, on some operational maps, further parts of the data present a low amplitude. Beyond the electromagnetic horizon of the radar, the absence of reflectors gives a homogeneous area
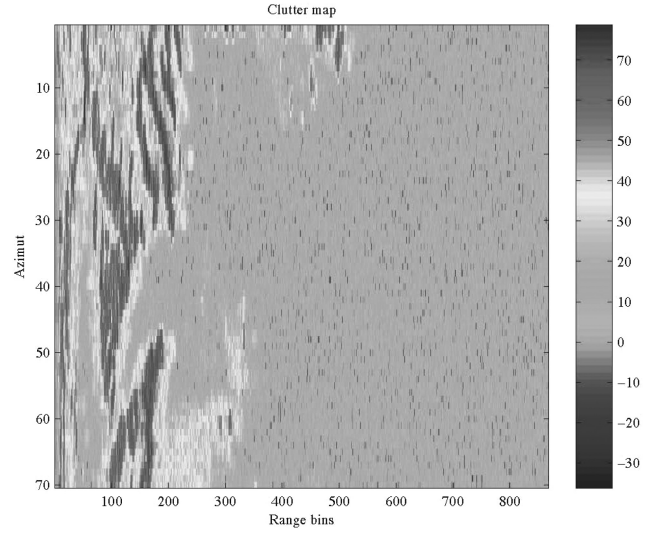

Fig. 1.   Ground clutter data level (in dB) corresponding to the first pulse.

of data, characterized as Gaussian thermal noise. A statistical selection of these data allows us to obtain experimental Gaussian noise to test our detection algorithm.

For that purpose, the well-known goodness-of-fit test of Kolmogorov-Smirnov (KS) is widely used [25]. This test verifies the adequacy of a given data sample to a Gaussian distributed sample $\mathcal{N}(\mu; \sigma)$. In order to obtain a homogeneous area of data, the KS test is applied successively on little blocks of data. With this test, the non-Gaussian data are rejected but the obtained map is lacunar. Indeed, the original clutter map presents a particular structure where there are horizontal bands corresponding to constant azimuths of the radar. The transitions between these bands show a significant difference of the mean of the data and a consequence is that the KS test is then inefficient. This is also the case for another goodness-of-fit test like Anderson-Darling [25].

In order to get a round this problem, a robust algorithm using connectedness of the data is developed. The idea is to include in the Gaussian area all the little blocks of supposed non-Gaussian data when they are not connected with the main non-Gaussian area. All the little blocks of data which are Gaussian but not characterized as Gaussian because of the nonhomogeneity of the KS test are now included in the main Gaussian area. We obtain with this method a wide area of Gaussian homogeneous data. In Fig. 2(a), we present the Gaussian area selected by the statistical study of the entire map. The Gaussian area is colored in red and the non-Gaussian area is in blue. This map confirms that only Gaussian thermal noise is present on the radioelectric horizon of the radar. In terms of experimental data, we present in Fig. 2(b) the clutter map with only Gaussian data extracted. The similar
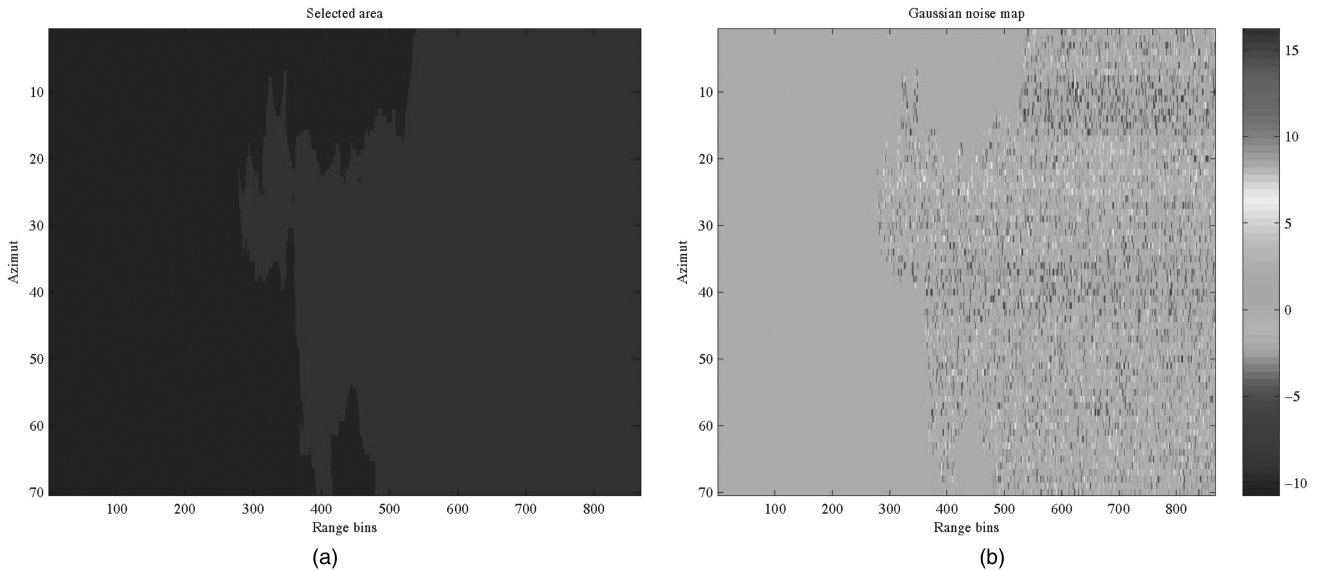
Fig. 2. Selection of Gaussian area in data presented in Fig. 1. (a) Binary area selected for Gaussian data extraction (Gaussian area in red and non-Gaussian in blue). (b) Gaussian map (in dB) corresponding to Gaussian selection and extracted from entire map.

color map as in Fig. 1 allows to verify the adequacy between original and extracted data.

Once Gaussian data have been extracted from the entire clutter map, we present the classical performance of this detector. In Fig. 3(a) and Fig. 4(a), the PFAs with respect to detection threshold are presented. The theoretical relations for the OGD, the AMF, and the PS-AMF are compared with the experimental relation (AMF and PS-AMF) in order to confirm the validity of the statistical study. Experimental curves are determined by Monte-Carlo counting, moving a (5×3) and (5×5) CFAR mask with a different number of simulations ($n$simu). The theoretical relation is then validated. In Fig. 3(b) and 4(b), we present the probability of detection versus signal-to-noise ratio (SNR) in order to verify and to quantify the improvement in terms of detection for the PS-AMF compared with the AMF. However these figures show the benefit of taking into account the persymmetric structure of the CCM in the Gaussian case.

B. Non-Gaussian Experiments

In the context of non-Gaussian clutter, Conte and De Maio in [5] and [6] have proposed two detectors derived, respectively, from the GLRT with some different estimators: the P-ANMF and the RP-ANMF. In [5] the persymmetry property is only used to separate their original set of secondary data $\mathbf{n}_k$ into two new uncorrelated and then independent sets of data $\mathbf{r}_{ek}$ and $\mathbf{r}_{ok}$, in order to render the detector matrix-CFAR and improve the performance in terms of detection. These new vectors have the same size as the original, and share the same texture. Their speckle components are IID and zero-mean complex Gaussian vectors. These new sets of secondary data

allow the introduction of their new estimator for the CCM:

$$\hat{\Sigma} = \frac{1}{K} \sum_{k=1}^{K} \frac{\mathbf{r}_{ek}\mathbf{r}_{ek}^{\mathrm{H}}}{(|\mathbf{r}_{ok}\mathbf{r}_{ok}^{\mathrm{H}}|)_{i,i}} \qquad (39)$$

where $(\mathbf{A})_{i,i}$ stands for any (i,i)th element of the matrix $\mathbf{A}$.

The previous estimator is then replaced in the classical GLRT-LQ given by (7) which leads to the P-ANMF detector defined as

$$\Lambda_{\text{P-ANMF}} = \frac{|\mathbf{p}^{\mathrm{H}}\hat{\Sigma}^{-1}\mathbf{x}|^2}{(\mathbf{p}^{\mathrm{H}}\hat{\Sigma}^{-1}\mathbf{p})(\mathbf{x}^{\mathrm{H}}\hat{\Sigma}^{-1}\mathbf{x})} \underset{H_0}{\overset{H_1}{\gtrless}} \lambda_{\text{P-ANMF}}. \qquad (40)$$

In [6], the same method is used to define two set of secondary data $\mathbf{r}_{ek}$ and $\mathbf{r}_{ok}$ and the FP matrix estimator $\hat{\Sigma}_{(\text{inf})}$ is found by using the recursive procedure:

$$\hat{\Sigma}_{(t+1)} = \frac{N}{K} \sum_{k=1}^{K} \frac{\mathbf{r}_{ek}\mathbf{r}_{ek}^{\mathrm{H}}}{\mathbf{r}_{ek}^{\mathrm{H}}(\hat{\Sigma}_{(t)})^{-1}\mathbf{r}_{ek}} \qquad (41)$$

with starting point:

$$\hat{\Sigma}_{(0)} = \frac{1}{K} \sum_{1}^{K} \frac{\mathbf{r}_{ek}\mathbf{r}_{ek}^{\mathrm{H}}}{(|\mathbf{Tr}_{ok}\mathbf{r}_{ok}^{\mathrm{H}}\mathbf{T}^{\mathrm{H}}|)_{i,i}}. \qquad (42)$$

This estimator is next replaced in the GLRT-LQ (7) to provide the RP-ANMF:

$$\Lambda_{\text{RP-ANMF}} = \frac{|\mathbf{p}^{\mathrm{H}}\hat{\Sigma}_{(\text{inf})}^{-1}\mathbf{x}|^2}{(\mathbf{p}^{\mathrm{H}}\hat{\Sigma}_{(\text{inf})}^{-1}\mathbf{p})(\mathbf{x}^{\mathrm{H}}\hat{\Sigma}_{(\text{inf})}^{-1}\mathbf{x})} \underset{H_0}{\overset{H_1}{\gtrless}} \lambda_{\text{RP-ANMF}}. $$

$$(43)$$

Please note that as stated in [20], the solution $\hat{\Sigma}^{(\text{inf})}$ of the implicit FP matrix equation is unique and does not depend on the starting point.
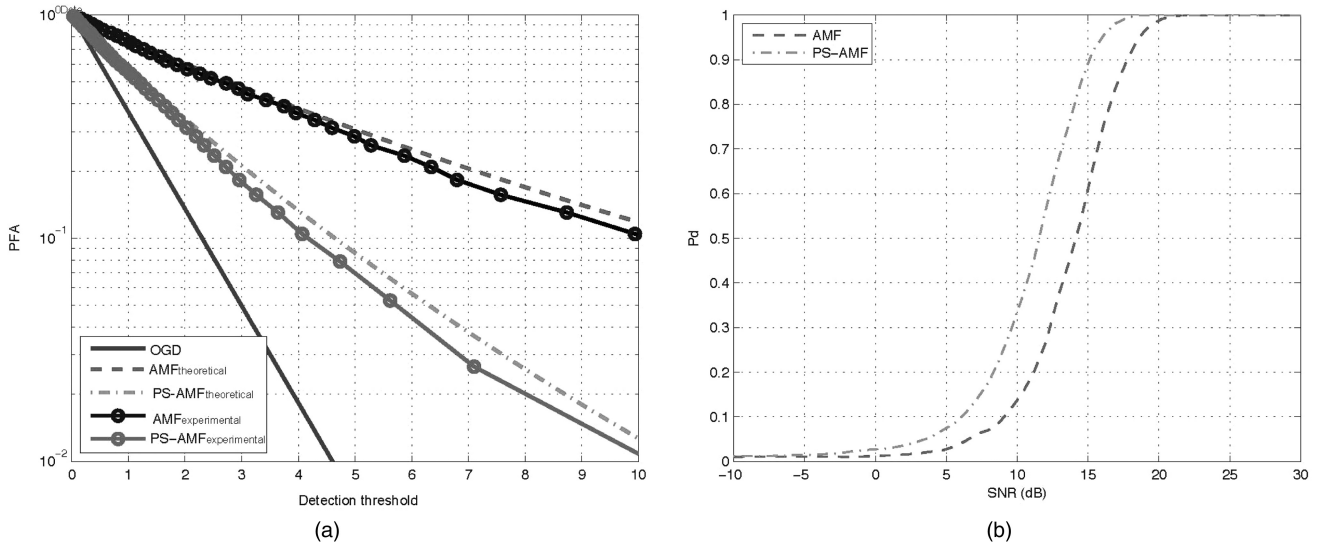
Fig. 3. Comparison between performance of detectors for $P_{\text{fa}} = 10^{-2}$, $m = 8$, $K = 14$. (a) Theoretical and experimental PFA-threshold curves for various Gaussian detectors. (b) Probability of detection versus SNR for AMF and PS-AMF.

Fig. 4. Comparison between performance of detectors for $P_{\text{fa}} = 10^{-2}$, $m = 8$, $K = 24$. (a) Theoretical and experimental PFA-threshold curves for various Gaussian detectors. (b) Probability of detection versus SNR for the AMF and PS-AMF.
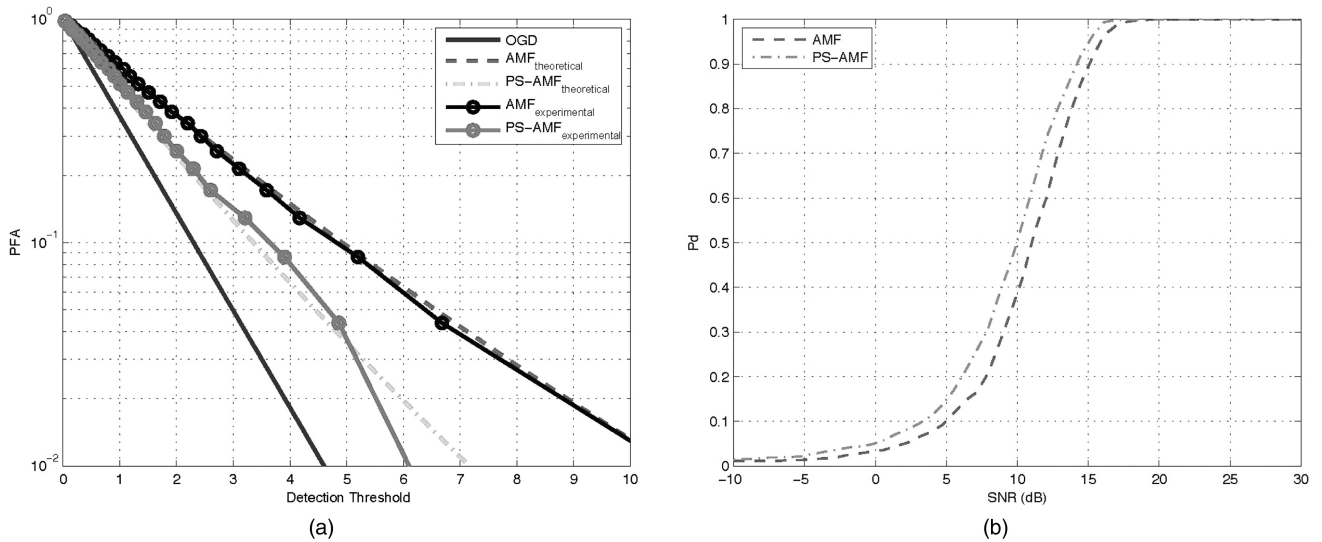
In order to compare all these detectors (GLRT-LQ with $\mathbf{M}$ known, generalized likelihood ratio test-sample covariance matrix (GLRT-SCM) with the classical SCM, GLRT-FP, GLRT-PFP, P-ANMF, and RP-ANMF), we present in Fig. 5(a) the PFA versus the detection threshold for all these detectors and in Fig. 5(b), the probability of detection versus the SNR. The simulated impulsive clutter is in this case chosen to be K-distributed [26]:

$$f_x(x) = \frac{2}{a\Gamma(\nu + 1)}\left(\frac{x}{2a}\right)^{\nu+1} K_\nu\left(\frac{x}{a}\right)$$

where $\Gamma(.)$ is the standard Gamma function [13], K_ν is the modified Bessel function of order ν [13], and where a and ν are constant positive parameters.

These figures show the improvement in terms of detection of the RP-ANMF on the conventional GLRT-SCM (which is not efficient on non-Gaussian data) but also the improvement of the GLRT-PFP on all the other detectors. Moreover, theoretical results based on the asymptotic Wishart distributions of $\hat{\mathbf{R}}_{\text{FP}}$ and $\hat{\mathbf{R}}_{\text{PFP}}$ (circle lines) are displayed. It can be noticed that the simulated results are in very good agreement with the theory.

Similar analyses performed on experimental sea-clutter data give the same conclusion. Fig. 6(a) and Fig. 6(b) show the sea clutter signal (range bins versus pulse repetition interval and range-Doppler) collected by the operational over the horizon radar from the French Aerospace Lab (ONERA) illumining the Atlantic ocean, and its associated range-Doppler
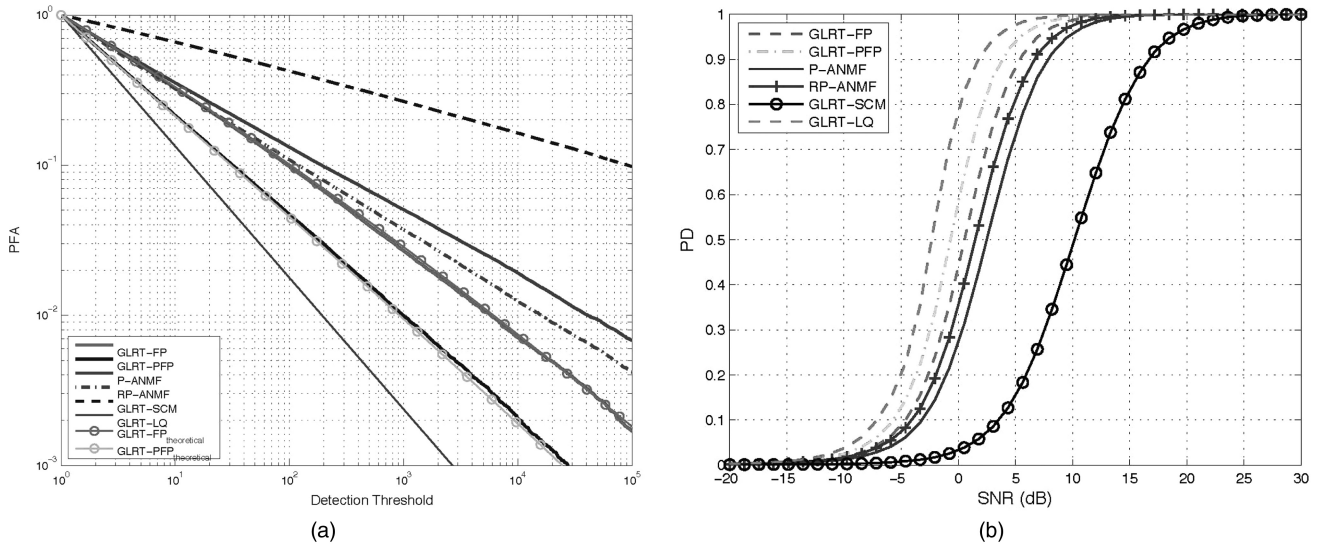
Fig. 5. Comparison between radar performance for various non-Gaussian detectors in simulated K-distributed clutter characterized by its parameter ν with $P_{fa} = 10^{-3}$, $m = 8$, $K = 16$, $\nu = 0.2$. (a) Theoretical and experimental PFA-threshold curves for various non-Gaussian detectors. (b) Probability of detection versus SNR for various non-Gaussian detectors.
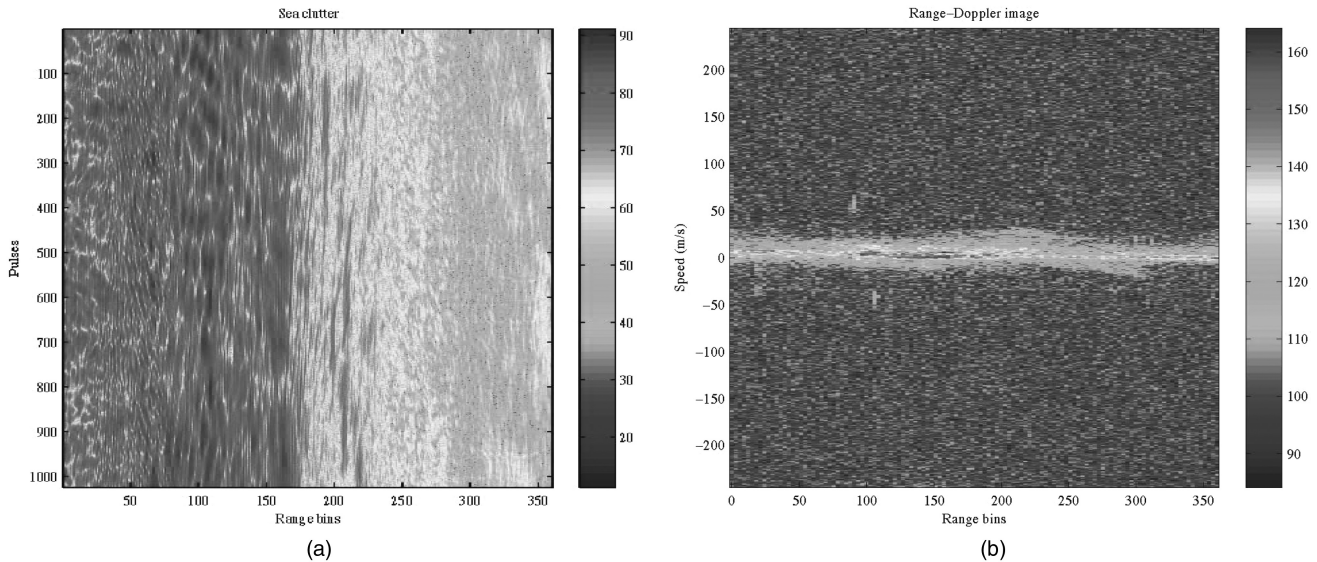

Fig. 6. Atlantic Ocean sea clutter data collected by the ONERA Over the horizon radar nostradamus. (a) Sea clutter data from over-the-horizon radar. (b) Range-Doppler image of Atlantic Ocean sea clutter.

image. In this context, we use a set of $m = 8$ pulses of the signal on the entire range bins group and $K = 16$ reference range bins to estimate the CCM. Fig. 7(a) and Fig. 7(b) show the improvement in detection performance on these data and the agreement between theoretical (circle line) and practical (solid line) results.

V. CONCLUSION

In the radar detection framework, estimation of the CCM is a major procedure in the detection process. In many applications, since this matrix commonly exhibits a particular structure, we therefore introduced in this paper two adaptive detection tests which take into account the widespread persymmetric structure of the CCM. In both contexts of Gaussian and non-Gaussian environments, we have presented and analyzed new detectors based on a modified estimator of the CCM.

Under Gaussian assumption, the CCM estimator is developed based on the ML procedure. The analytical distribution and some statistical properties of the corresponding detector, called the PS-AMF, have been established. These results are important since they enable a theoretical regulation of the false alarm, which is essential in the radar detection process.

The second detector is an extended version of the GLRT-LQ. It has been derived in the case of
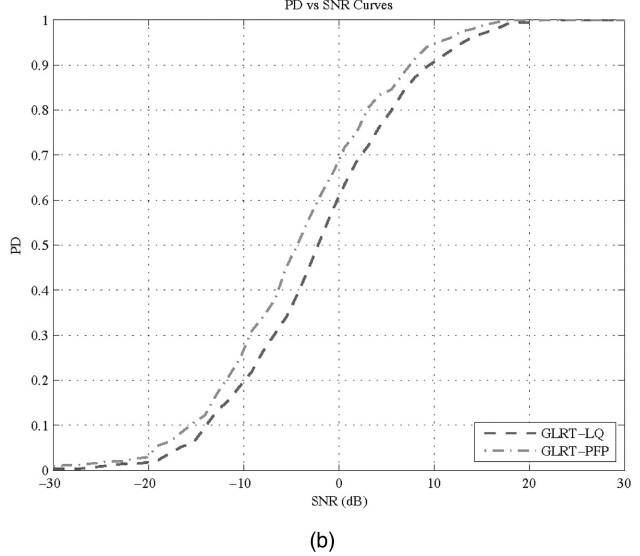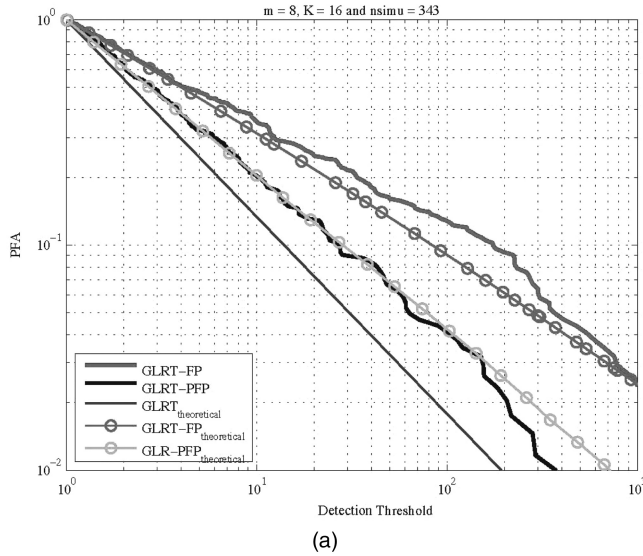
Fig. 7. Comparison between radar performance for various non-Gaussian detectors in sea clutter data for $P_{\text{fa}} = 10^{-2}$, $m = 8$, $K = 16$. (a) Theoretical and experimental PFA-threshold curves for various non-Gaussian detectors. (b) Probability of detection versus SNR for GLRT-FP and GLRT-PFP.

persymmetric non-Gaussian clutter modeled by SIRVs. After a transformation of the detection scheme, we have proposed an improved covariance matrix estimator, the PFP estimator. Its complete statistical analyses have exhibited good statistical performance. Moreover the corresponding GLRT-PFP detector has shown a wide improvement in terms of detection performance, as compared with the classical detectors.

Finally, all these theoretical results have been validated on simulations for both Gaussian and non-Gaussian environments. Moreover, we have shown the validity and the good agreement between the theoretical and the experimental results, on both real ground and sea clutter data. Furthermore, the performance of the proposed detectors and the classical ones have been compared on these real data which highlight the improved performance of the former. These analysis have demonstrated the relevance and the advantage of exploiting the CCM structure.

ACKNOWLEDGMENT

APPENDIX

A. Proof of Proposition 3

We use in this derivation the Bartlett matrix decomposition [27]. Let us set $\mathbf{e}_1 = (1, 0, \ldots, 0)^{\text{T}}$, $\mathbf{R} = \mathbf{R}^{1/2}\mathbf{R}^{\text{T}/2}$ a factorization of $\mathbf{R}$ and $\mathbf{Q}$ a real unitary matrix such that $\mathbf{Q}\mathbf{R}^{-1/2}\mathbf{s} = (\mathbf{s}^{\text{T}}\mathbf{R}^{-1}\mathbf{s})^{1/2}\mathbf{e}_1$. Note that

the last equation is possible with $\mathbf{Q}$ real since $\mathbf{s}$ is itself real. Let us set

$$\hat{\mathbf{W}} = 2K\mathbf{Q}\mathbf{R}^{-1/2}\hat{\mathbf{R}}_P\mathbf{R}^{-\text{T}/2}\mathbf{Q}^{\text{T}} \quad \text{and} \quad \mathbf{z} = \mathbf{Q}\mathbf{R}^{-1/2}\mathbf{x}.$$

$\hat{\mathbf{W}}$ is real Wishart distributed with $2K$ degrees of freedom and parameter matrix $\mathbf{I}_m$, $\mathbf{z} \sim \mathcal{CN}(\mathbf{0}, \mathbf{I}_m)$. Then, the test statistic $\Lambda_{\text{PS-AMF}}$ (25) is equal to

$$\Lambda_{\text{PS-AMF}} = \frac{|\mathbf{s}^{\text{T}}\hat{\mathbf{R}}_P^{-1}\mathbf{x}|^2}{\mathbf{s}^{\text{T}}\hat{\mathbf{R}}_P^{-1}\mathbf{s}}$$

$$= \frac{|\mathbf{s}^{\text{T}}\mathbf{R}^{-\text{T}/2}\mathbf{Q}^{\text{T}}(\mathbf{Q}\mathbf{R}^{-1/2}\hat{\mathbf{R}}_P\mathbf{R}^{-\text{T}/2}\mathbf{Q}^{\text{T}})^{-1}\mathbf{Q}\mathbf{R}^{-1/2}\mathbf{x}|^2}{\mathbf{s}^{\text{T}}\mathbf{R}^{-\text{T}/2}\mathbf{Q}^{\text{T}}(\mathbf{Q}\mathbf{R}^{-1/2}\hat{\mathbf{R}}_P\mathbf{R}^{-\text{T}/2}\mathbf{Q}^{\text{T}})^{-1}\mathbf{Q}\mathbf{R}^{-1/2}\mathbf{s}}$$

$$= 2K\frac{|\mathbf{e}_1^{\text{T}}\hat{\mathbf{W}}^{-1}\mathbf{z}|^2}{\mathbf{e}_1^{\text{T}}\hat{\mathbf{W}}^{-1}\mathbf{e}_1} \tag{44}$$

which may be rewritten, for our statistical analysis, as

$$\Lambda_{\text{PS-AMF}} = 2Kba \tag{45}$$

where

$$a = \frac{|\mathbf{e}_1^{\text{T}}\hat{\mathbf{W}}^{-1}\mathbf{x}|^2}{\mathbf{e}_1^{\text{T}}\hat{\mathbf{W}}^{-2}\mathbf{e}_1}, \qquad b = \left(\frac{\mathbf{e}_1^{\text{T}}\hat{\mathbf{W}}^{-2}\mathbf{e}_1}{\mathbf{e}_1^{\text{T}}\hat{\mathbf{W}}^{-1}\mathbf{e}_1}\right).$$

We show that a and b are independent and we derive their statistical distribution. Let us first investigate the distribution of a. By introducing the unitary vector $\mathbf{v}$, defined by

$$\mathbf{v} = \frac{1}{(\mathbf{e}_1^{\text{T}}\hat{\mathbf{W}}^{-2}\mathbf{e}_1)^{1/2}}\hat{\mathbf{W}}^{-1}\mathbf{e}_1$$

a may be rewritten as

$$a = |\mathbf{v}^{\text{T}}\mathbf{x}|^2.$$

It follows that the conditional distribution of $2a$ given $\hat{\mathbf{W}}$ is a chi-square distribution with 2 degrees of

freedom denoted by χ_2^2. This distribution does not involve $\hat{\mathbf{W}}$, and

$$a \sim \tfrac{1}{2}\chi_2^2 \qquad (46)$$

is therefore independent of $\hat{\mathbf{W}}$ and consequently of b.

Now, to derive the pdf of b, we use the Bartlett matrix decomposition $\hat{\mathbf{W}} = \mathbf{U}.\mathbf{U}^{\mathrm{T}}$ where $\mathbf{U} = (u_{ij})_{1 \le i \le j \le m}$ is an upper triangular matrix whose random elements are independent and distributed as

$$u_{i,i}^2 \sim \chi_{2K+i-m}^2 \qquad \text{and} \qquad u_{i,j} \sim \mathcal{N}(0,1) \quad \text{for} \quad i < j.$$

Let $u'_{i,j}$ be the elements of the matrix $\mathbf{U}^{-1}$ which is itself upper-triangular. By noticing that $\mathbf{U}^{-1}\mathbf{e}_1 = u'_{1,1}\mathbf{e}_1$, we have

$$
\begin{aligned}
b &= \frac{\mathbf{e}_1^{\mathrm{T}}\hat{\mathbf{W}}^{-2}\mathbf{e}_1}{\mathbf{e}_1^{\mathrm{T}}\hat{\mathbf{W}}^{-1}\mathbf{e}_1} \\
&= \frac{\mathbf{e}_1^{\mathrm{T}}\mathbf{U}^{-\mathrm{T}}\mathbf{U}^{-1}\mathbf{U}^{-\mathrm{T}}\mathbf{U}^{-1}\mathbf{e}_1}{\mathbf{e}_1^{\mathrm{T}}\mathbf{U}^{-\mathrm{T}}\mathbf{U}^{-1}\mathbf{e}_1} \\
&= \|\mathbf{e}^{\mathrm{T}}\mathbf{U}^{-1}\|^2 \\
&= \sum_{j=1}^{m} u_{1,j}'^2.
\end{aligned}
\qquad (47)
$$

We are thus lead to investigate the distribution of the squared norm of the first row of $\mathbf{U}^{-1}$. Let $\mathbf{u}'_{1,k}$ be the kth order vector whose components are the k first elements of the first row of $\mathbf{U}^{-1}$, and $\mathbf{u}_{i,j}$ be the ith order vector the components of which are the i first elements of the jth column of $\mathbf{U}$. The definition of $\mathbf{U}^{-1}$, i.e., $\mathbf{U}^{-1}\mathbf{U} = \mathbf{I}_m$, allows to determine recursively its elements according to

$$u'_{1,1} = u_{1,1}^{-1}$$

and

$$u'_{1,k+1} = \frac{-\mathbf{u}_{1,k}'^{\mathrm{T}}\mathbf{u}_{k,k+1}}{u_{k+1,k+1}} \qquad \text{for} \quad 1 \le k < m.$$

It follows that $\mathbf{u}'_{1,k}$ is independent of the $u_{i,j}$s for $j > k$. Now we have from the above equation:

$$
\begin{aligned}
u_{1,k+1}'^2 &= \frac{|\mathbf{u}_{1,k}'^{\mathrm{T}}\mathbf{u}_{k,k+1}|^2}{u_{k+1,k+1}^2} \\
&= \frac{|\mathbf{u}_{1,k}'^{\mathrm{T}}\mathbf{u}_{k,k+1}|^2}{\|\mathbf{u}'_{1,k}\|^2}\frac{\|\mathbf{u}'_{1,k}\|^2}{u_{k+1,k+1}^2} \\
&= \alpha_k \frac{\|\mathbf{u}'_{1,k}\|^2}{u_{k+1,k+1}^2}.
\end{aligned}
\qquad (48)
$$

The conditional distribution of α_k given $\mathbf{u}'_{1,k}$ is a chi-square distribution with 1 degree of freedom denoted by χ_1^2. This distribution does not involve $\mathbf{u}'_{1,k}$ and $\alpha_k \sim \chi_1^2$ is therefore independent of $\mathbf{u}'_{1,k}$. Moreover, α_k is independent of $u_{i,j}$ for i and $j >$

k. Now, notice from (48) that $b = \|\mathbf{u}'_{1,m}\|^2$. Since $\|\mathbf{u}'_{1,m}\|^2 = \|\mathbf{u}'_{1,m-1}\|^2 + u_{1,m}'^2$, one has therefore:

$$
\begin{aligned}
b &= \|\mathbf{u}'_{m-1}\|^2\left(1 + \frac{\alpha_{m-1}}{u_{m,m}^2}\right) \\
&= \frac{1}{u_{1,1}^2}\prod_{k=2}^{m}\left(1 + \frac{\alpha_{k-1}}{u_{k,k}^2}\right)
\end{aligned}
\qquad (49)
$$

where the α_ks are independent, independent of the $u_{k,k}^2$s, and χ_1^2-distributed. Since

$$\left(1 + \frac{\alpha_{k-1}}{u_{k,k}^2}\right)^{-1} \sim \beta_1\left(\frac{2K-m+k}{2},\frac{1}{2}\right)$$

we have from [28]

$$
\begin{aligned}
b &= \frac{1}{u_{1,1}^2}\frac{1}{\prod_{k=2}^{m}\beta_1\left(\dfrac{2K-m+k}{2},\dfrac{1}{2}\right)} \\
&\sim \frac{1}{\chi_{2K-m+1}^2}\frac{1}{\beta_1\left(\dfrac{2K-m+2}{2},\dfrac{m-1}{2}\right)}
\end{aligned}
\qquad (50)
$$

where the β_1s are independent (first kind) Beta distributed random variables. Finally we obtain from (45), (46), and (49):

$$\Lambda_{\text{PS-AMF}} \sim K\frac{\chi_2^2}{\chi_{2K-m+1}^2}\frac{1}{\beta_1\left(\dfrac{2K-m+2}{2},\dfrac{m-1}{2}\right)} \qquad (51)$$

which can be rewritten in terms of an F-distributed random variable:

$$
\begin{aligned}
\Lambda_{\text{PS-AMF}} \sim {}& K\frac{2}{2K-m+1}F(2,2K-m+1) \\
&\times \frac{1}{\beta_1\left(\dfrac{2K-m+2}{2},\dfrac{m-1}{2}\right)}.
\end{aligned}
\qquad (52)
$$

Let us now derive the PFA-threshold relation. From [13, p. 946],

$$
\begin{aligned}
\text{PFA} &= \Pr(\Lambda_{\text{PS-AMF}} > \lambda) \\
&= \Pr\left(F(2,2K-m+1) > \frac{2K-m+1}{2}\frac{\lambda}{K}\beta_1\right. \\
&\qquad\left. \times\left(\frac{2K-m+2}{2},\frac{m-1}{2}\right)\right) \\
&= \int_0^1 \left(\frac{1}{1+\dfrac{\lambda}{K}x}\right)^{(2K-m+1)/2} f_{\nu1,\nu2}(x)\,dx
\end{aligned}
\qquad (53)
$$

where $f_{\nu1,\nu2}$ is the pdf of a first kind beta random variable with parameters $\nu1 = (2K-m+2)/2$ and

$\nu 2 = (m-1)/2$. We finally obtain

$$
\text{PFA} = \frac{1}{B\left(\dfrac{2K-m+2}{2}, \dfrac{m-1}{2}\right)} \int_0^1 \left(\frac{1}{1+\dfrac{\lambda}{K}.x}\right)^{(2K-m+1)/2}
$$

$$
\times x^{((2K-m+2)/2)-1}(1-x)^{((m-1)/2)-1} dx \qquad (54)
$$

which may be expressed in terms of the hypergeometric function [13, p. 558]

$$
P_{\text{fa}} = {}_2F_1\left(\frac{2K-m+1}{2}, \frac{2K-m+2}{2}; \frac{2K+1}{2}; -\frac{\lambda}{K}\right). \qquad (55)
$$

The negative derivative of P_{fa} with respect to λ yields the pdf of $\Lambda_{\text{PS-AMF}}$. By using the expression of the derivative of hypergeometric functions given in [13, p. 557], we obtain (27) which concludes the proof.

B. Proof of Proposition 6

From Proposition 5, $\Lambda_{\text{GLRT-PFP}}$ has the same asymptotic distribution as

$$
\Lambda = \frac{|\mathbf{e}_1^{\mathrm{T}}\hat{\mathbf{W}}^{-1}\mathbf{w}|^2}{(\mathbf{e}_1^{\mathrm{T}}\hat{\mathbf{W}}^{-1}\mathbf{e}_1)(\mathbf{w}^{\mathrm{H}}\hat{\mathbf{W}}^{-1}\mathbf{w})}
$$

$$
= \frac{\left|\mathbf{e}_1^{\mathrm{T}}\hat{\mathbf{W}}^{-1}\left(\sqrt{2}\mathbf{w}\right)\right|^2}{(\mathbf{e}_1^{\mathrm{T}}\hat{\mathbf{W}}^{-1}\mathbf{e}_1)\left(\sqrt{2}\mathbf{w}^{\mathrm{H}}\hat{\mathbf{W}}^{-1}\sqrt{2}\mathbf{w}\right)} \qquad (56)
$$

where $(\sqrt{2}\mathbf{w}) = \mathbf{w}_1 + i\mathbf{w}_2$ with $\mathbf{w}_1$ and $\mathbf{w}_2$ uncorrelated and $\mathcal{N}(\mathbf{0},\mathbf{I})$ distributed.

Thus

$$
\Lambda = \frac{|\mathbf{e}_1^{\mathrm{T}}\hat{\mathbf{W}}^{-1}\mathbf{w}_1|^2 + |\mathbf{e}_1^{\mathrm{T}}\hat{\mathbf{W}}^{-1}\mathbf{w}_2|^2}{(\mathbf{e}_1^{\mathrm{T}}\hat{\mathbf{W}}^{-1}\mathbf{e}_1)(\mathbf{w}_1^{\mathrm{T}}\hat{\mathbf{W}}^{-1}\mathbf{w}_1 + \mathbf{w}_2^{\mathrm{T}}\hat{\mathbf{W}}^{-1}\mathbf{w}_2)}.
$$

For large K, $\hat{\mathbf{W}}$ is real Wishart distributed with $K' = (m/(m+1))2K$ degrees of freedom. The vectors $\mathbf{w}_1$ and $\mathbf{w}_2$ can be decomposed on an orthonormal vectors triplet $(\mathbf{e}_1, \mathbf{f}_2, \mathbf{f}_3)$:

$$
\mathbf{w}_1 = \alpha_1\mathbf{e}_1 + \alpha_2\mathbf{f}_2
$$

$$
\mathbf{w}_2 = \beta_1\mathbf{e}_1 + \beta_2\mathbf{f}_2 + \beta_3\mathbf{f}_3
$$

where α_1, β_1 and β_2 are $\mathcal{N}(0,1)$ distributed, α_2^2 is χ^2_{m-1} distributed and β_3^2 is χ^2_{m-2} distributed. Moreover α_1, α_2, β_1, β_2, β_3 are independent and independent of $(\mathbf{f}_2, \mathbf{f}_3)$.

Let $(\mathbf{e}_1, \mathbf{e}_2, \ldots, \mathbf{e}_m)$ be the canonical basis. Using an appropriate rotation $\mathbf{G}$ such that $\mathbf{G}(\mathbf{e}_1, \mathbf{f}_2, \mathbf{f}_3) = (\mathbf{e}_1, \mathbf{e}_2, \mathbf{e}_3)$, we have

$$
\mathbf{G}\mathbf{w}_1 = \alpha_1\mathbf{e}_1 + \alpha_2\mathbf{e}_2
$$

$$
= \mathbf{v}_1 \qquad (57)
$$

$$
\mathbf{G}\mathbf{w}_2 = \beta_1\mathbf{e}_1 + \beta_2\mathbf{e}_2 + \beta_3\mathbf{e}_3
$$

$$
= \mathbf{v}_2 \qquad (58)
$$

and Λ can be rewritten as

$$
\Lambda = \frac{|\mathbf{e}_1^{\mathrm{T}}\hat{\mathbf{Z}}^{-1}\mathbf{v}_1|^2 + |\mathbf{e}_1^{\mathrm{T}}\hat{\mathbf{Z}}^{-1}\mathbf{v}_2|^2}{(\mathbf{e}_1^{\mathrm{T}}\hat{\mathbf{Z}}^{-1}\mathbf{e}_1)(\mathbf{v}_1^{\mathrm{T}}\hat{\mathbf{Z}}^{-1}\mathbf{v}_1 + \mathbf{v}_2^{\mathrm{T}}\hat{\mathbf{Z}}^{-1}\mathbf{v}_2)} \qquad (59)
$$

where $\hat{\mathbf{Z}} = \mathbf{G}\hat{\mathbf{W}}\mathbf{G}^{\mathrm{T}}$.

Conditionally (and unconditionally) to $\mathbf{G}$, $\hat{\mathbf{Z}}$ is Wishart distributed with K' degrees of freedom and parameter matrix $\mathbf{I}$. Let $\hat{\mathbf{Z}} = \mathbf{L}^{\mathrm{T}}\mathbf{L}$ be the Bartlett's decomposition of $\hat{\mathbf{Z}}$ [27] where $\mathbf{L} = (l_{i,j})_{1 \leq i \leq j \leq m}$ is a lower triangular matrix whose non-zeros random elements are independent and distributed as

$$
l_{i,i}^2 \sim \chi^2_{K'+i-m} \qquad \text{and} \qquad l_{i,j} \sim \mathcal{N}(0,1) \quad \text{for} \quad i > j.
$$

Let $l'_{i,j}$ be the elements of the matrix $\mathbf{L}^{-1}$ which is lower-triangular itself. The following elements of $\mathbf{L}^{-1}$ are involved in (59):

$$
l'_{11} = \frac{1}{l_{11}}, \qquad l'_{22} = \frac{1}{l_{22}}, \qquad l'_{21} = -\frac{l_{21}}{l_{11}l_{22}}
$$

$$
l'_{33} = \frac{1}{l_{33}}, \qquad l'_{32} = -\frac{l_{32}}{l_{22}l_{33}}, \qquad l'_{31} = -\frac{1}{l_{11}}\left(\frac{l_{31}}{l_{33}} - \frac{l_{32}l_{21}}{l_{22}l_{33}}\right). \qquad (60)
$$

From (59), we define

$$
\alpha = \frac{|\mathbf{e}_1^{\mathrm{T}}\hat{\mathbf{Z}}^{-1}\mathbf{v}_1|^2 + |\mathbf{e}_1^{\mathrm{T}}\hat{\mathbf{Z}}^{-1}\mathbf{v}_2|^2}{\mathbf{e}_1^{\mathrm{T}}\hat{\mathbf{Z}}^{-1}\mathbf{e}_1}
$$

which can be rewritten as

$$
\alpha = \frac{|\mathbf{e}_1^{\mathrm{T}}\mathbf{L}^{-1}\mathbf{L}^{-\mathrm{T}}\mathbf{G}\mathbf{w}_1|^2 + |\mathbf{e}_1^{\mathrm{T}}\mathbf{L}^{-1}\mathbf{L}^{-\mathrm{T}}\mathbf{G}\mathbf{w}_2|^2}{\mathbf{e}_1^{\mathrm{T}}\mathbf{L}^{-1}\mathbf{L}^{-\mathrm{T}}\mathbf{e}_1}
$$

$$
= (\alpha_1 l'_{11} + \alpha_2 l'_{21})^2 + (\beta_1 l'_{11} + \beta_2 l'_{21} + \beta_3 l'_{31})^2
$$

and

$$
\beta = \mathbf{v}_1^{\mathrm{T}}\hat{\mathbf{Z}}^{-1}\mathbf{v}_1 + \mathbf{v}_2^{\mathrm{T}}\hat{\mathbf{Z}}^{-1}\mathbf{v}_2
$$

which can be rewritten as

$$
\beta = \mathbf{v}_1^{\mathrm{T}}\mathbf{L}^{-1}\mathbf{L}^{-\mathrm{T}}\mathbf{v}_1 + \mathbf{v}_2^{\mathrm{T}}\mathbf{L}^{-1}\mathbf{L}^{-\mathrm{T}}\mathbf{v}_2
$$

$$
= \alpha + (l'_{22}\alpha_2)^2 + (l'_{22}\beta_2 + l'_{32}\beta_3)^2 + (l'_{33}\beta_3)^2.
$$

We deduce that $\Lambda = \alpha/\beta = F/(1+F)$ with

$$
F = \frac{(\alpha_1 l'_{11} + \alpha_2 l'_{21})^2 + (\beta_1 l'_{11} + \beta_2 l'_{21} + \beta_3 l'_{31})^2}{(l'_{22}\alpha_2)^2 + (l'_{22}\beta_2 + l'_{32}\beta_3)^2 + (l'_{33}\beta_3)^2}
$$

$$
= \frac{(\alpha_1 l_{22} - \alpha_2 l_{21})^2 + \left(\beta_1 l_{22} - \beta_2 l_{21} - \beta_3\dfrac{l_{31}}{l_{33}}l_{22} + \dfrac{l_{32}l_{21}}{l_{33}}\beta_3\right)^2}{(l_{11}\alpha_2)^2 + \left(\dfrac{l_{11}l_{22}}{l_{33}}\beta_3\right)^2 + l_{11}^2\left(\beta_2 - \dfrac{\beta_3}{l_{33}}l_{32}\right)^2}. \qquad (61)
$$

In this equation we have

$$\left(\beta_1 l_{22} - \beta_2 l_{21} - \beta_3 \frac{l_{31}}{l_{33}} l_{32} + \frac{l_{32} l_{21}}{l_{33}} \beta_3 \right)^2$$

$$= \left(l_{22} \left(\beta_1 - \frac{\beta_3}{l_{33}} l_{31} \right) - l_{21} \left(\beta_2 - \frac{\beta_3}{l_{33}} l_{32} \right) \right)^2$$

$$= \left(1 + \left(\frac{\beta_3}{l_{33}} \right)^2 \right) (l_{22} a - l_{21} b)^2 \qquad (62)$$

with

$$a = \frac{1}{\sqrt{1 + \left(\dfrac{\beta_3}{l_{33}} \right)^2}} \left(\beta_1 - \frac{\beta_3}{l_{33}} l_{31} \right)$$

$$b = \frac{1}{\sqrt{1 + \left(\dfrac{\beta_3}{l_{33}} \right)^2}} \left(\beta_2 - \frac{\beta_3}{l_{33}} l_{32} \right).$$

Conditionally to β_3 and l_{33}, a and b are independent and $\mathcal{N}(0,1)$ distributed. Since their distribution does not involve β_3 and l_{33}, a and b are also independent of β_3 and u_{33}.

By replacing it in (61), we finally obtain

$$F = \frac{(\alpha_1 l_{22} - \alpha_2 l_{21})^2 + \left(1 + \left(\dfrac{\beta_3}{l_{33}} \right)^2 \right) (a l_{22} - b l_{21})^2}{(\alpha_2 l_{11})^2 + \left(l_{11} l_{22} \dfrac{\beta_3}{l_{33}} \right)^2 + l_{11}^2 \left(1 + \left(\dfrac{\beta_3}{l_{33}} \right)^2 \right) b^2} \qquad (63)$$

where all the following random variables are independent and distributed according to

$$a, b, \alpha_1, l_{21} \sim \mathcal{N}(0,1), \qquad \alpha_2^2 \sim \chi_{m-1}^2, \qquad \beta_3^2 \sim \chi_{m-2}^2$$

$$l_{11}^2 \sim \chi_{K'-m+1}^2, \qquad l_{22}^2 \sim \chi_{K'-m+2}^2, \qquad l_{33}^2 \sim \chi_{K'-m+3}^2$$

with $K' = (m/(m+1))2K$ which concludes the proof.

REFERENCES

[1]   Burg, J. P., Luenberger, D. G., and Wenger, D. L.
        Estimation of structured covariance matrices.
        Proceedings of the IEEE, **70** (Sept. 1982), 963–974.

[2]   Fuhrmann, D. R.
        Application of Toeplitz covariance estimation to adaptive
        beamforming and detection.
        IEEE Transactions on Signal Processing, **39** (Oct. 1991),
        2194–2198.

[3]   Nitzberg, R. and Burke, J. R.
        Application of maximum likelihood estimation of
        persymmetric covariance matrices to adaptive detection.
        IEEE Transactions on Aerospace and Electronic Systems,
        AES-25 (Jan. 1980), 124–127.

[4]   Cai, L. and Wang, H.
        A persymmetric multiband GLR algorithm.
        IEEE Transactions on Aerospace and Electronic Systems,
        28, 3 (July 1992), 806–816.

[5]   Conte, E. and De Maio, A.
        Exploiting persymmetry for CFAR detection in
        compound-Gaussian clutter.
        IEEE Transactions on Aerospace and Electronic Systems,
        39 (Apr. 2003), 719–724.

[6]   Conte, E. and De Maio, A.
        Mitigation techniques for non-Gaussian sea clutter.
        IEEE Journal of Oceanic Engineering, **29** (Dec. 2003),
        284–302.

[7]   Gini, F. and Greco, M. V.
        Covariance matrix estimation for CFAR detection in
        correlated heavy tailed clutter.
        Signal Processing (special section on signal processing
        with heavy tailed distributions), **82** (Dec. 2002),
        1847–1859.

[8]   Conte, E., De Maio, A., and Ricci, G.
        Recursive estimation of the covariance matrix of a
        compound-Gaussian process and its application to
        adaptive CFAR detection.
        IEEE Transactions on Signal Processing, **50** (Aug. 2002),
        1908–1915.

[9]   Pailloux, G., et al.
        On persymmetric covariance matrices in adaptive
        detection.
        In *Proceedings of the IEEE International Conference on
        Acoustics, Speech and Signal Processing* (ICASSP 2008),
        Apr. 2008, 2305–2308.

[10]   Pailloux, G., et al.
        A SIRV-CFAR adaptive detector exploiting persymmetric
        clutter covariance structure.
        In *Proceedings of the IEEE Radar Conference 2008*
        (RadarCon2008), May 2008, 1139–1144.

[11]   Robey, F. C.
        A CFAR adaptive matched filter detector.
        IEEE Transactions on Aerospace and Electronic Systems,
        23 (Jan. 1992), 208–216.

[12]   Kraut, S., Scharf, L. L., and McWhorter, L. T.
        Adaptive subspace detector.
        IEEE Transactions on Signal Processing, **49** (Jan. 2001),
        1–16.

[13]   Abramovitch, M. and Stegun, I. A.
        Handbook of Mathematical Functions.
        National Bureau of Standards, Gaithersburg, MD, vol.
        AMS 55, June 1964.

[14]   Billingsley, J. B.
        Ground clutter measurement for surface sited radar.
        MIT Technical Report 780, Feb. 1993.

[15]   Yao, K.
        A representation theorem and its applications to
        spherically invariant random processes.
        IEEE Transactions on Information Theory, **IT-19** (Sept.
        1973), 600–608.

[16]   Rangaswamy, M., Weiner, D. D., and Ozturk, A.
        Non-Gaussian vector identification using spherically
        invariant random processes.
        IEEE Transactions on Aerospace and Electronic Systems,
        29 (Jan. 1993), 111–124.

[17]   Gini, F.
        Sub-optimum coherent radar detection in a mixture of
        K-distributed and Gaussian clutter.
        IEE Proceedings on Radar, Sonar Navigation, **144** (Feb.
        1997), 39–48.

[18]   Conte, E., Lops, M., and Ricci, G.
        Asymptotically optimum radar detection in
        compound-Gaussian clutter.
        IEEE Transactions on Aerospace and Electronic Systems,
        31 (Apr. 1995), 617–625.

[19] Scharf, L. L. and McWhorter, L. T.
Adaptive matched subspace detectors and adaptive
coherence estimators.
In *Proceedings of the 30th Asilomar Conference on Signals,
Systems, and Computers*, vol. 2, Nov. 1996, 1114–1117.

[20] Pascal, F., et al.
Covariance structure maximum likelihood estimates in
compound Gaussian noise: Existence and algorithm
analysis.
IEEE Transactions on Signal Processing, **56** (Jan. 2008),
34–38.

[21] Pascal, F., et al.
Performance analysis of covariance matrix estimate in
impulsive noise.
IEEE Transactions on Signal Processing, (June 2008),
2206–2217.

[22] Pascal, F., et al.
Constant false alarm rate detection in spherically invariant
random processes.
In *Proceedings of the European Signal Processing
Conference* (EUSIPCO-04), Vienna, Sept. 2004,
2143–2146.

[23] Van Trees, H. L.
*Detection, Estimation and Modulation Theory, Part IV:
Optimum Array Processing*.
Hoboken, NJ: Wiley, 2002.

[24] Pascal, F., et al.
On a SIRV-CFAR detector with radar experimentations in
impulsive noise.
In *Proceedings of the European Signal Processing
Conference* (EUSIPCO), Sept. 2006.

[25] Sheskin, D. J.
Parametric and non-parametric statistical procedures.
New York: Chapmann and Hall/CRC books, 2004.

[26] Raghavan, R. S.
A method for estimating parameters of K-distributed
clutter.
IEEE Transactions on Aerospace and Electronic Systems,
27 (Mar. 1991), 238–246.

[27] Muirhead, R. J.
Aspects of Multivariate Statistical Theory.
Hoboken, NJ: Wiley, 1982.

[28] Jambunathan, M. V.
Some properties of beta and gamma distributions.
The Annals of Mathematical Statistics, 25 (June 1954),
401–405.

Guilhem Pailloux (S'08) was born in le Chesnay, France, in 1983. He jointly
received the engineering degree form Ecole Nationale Supérieure d'Informatique,
Automatique et Mécanique (ENSIAME), Valenciennes, France and the master's
degree in science and technologie from University of Valenciennes in 2006.

He joined the Electomagnetic and Radar Division of the french Aerospace
Lab (ONERA) in 2007, in order to prepare his Ph.D degree in physics from the
University of Paris X. His research interests are estimation and detection theory
with application to radar and array processing.

Philippe Forster (M'89) was born in Brest, France, in 1960. He graduated from the Ecole Normale Supérieure de Cachan in 1983 with the Agrégation de Physique Appliquée degree, and from the Université de Rennes with a Ph.D. in electrical engineering in 1988.

From 1989 to 1992, he worked at Thomson Sintra ASM, doing research in signal processing for sonar applications. During that time he spent one year at Northeastern University, Boston, as a post-doctoral researcher. In September 1992, he joined the Conservatoire National des Arts et Métiers, Paris, as an assistant professor in Electrical Engineering, doing research in array processing for mobile communications. Since 2000, he is Professor of Electrical Engineering at the Université de Paris X, and member of the SATIE Laboratory at the Ecole Normale Supérieure de Cachan. His research interests are in array processing, detection and estimation theory.

Jean-Philippe Ovarlez (M'06) was born in Denain, France in 1963. He received jointly the engineering degree from Ecole Supérieure d'Electronique Automatique et Informatique (ESIEA), Paris, France and the Diplôme d'Etudes Approfondies degree in signal processing from University of Orsay (Paris XI), Orsay, France and the Ph.D. degree in physics from the University of Paris VI, Paris, France, in 1987 and 1992, respectively.

In 1992, he joined the Electromagnetic and Radar Division of the French Aerospace Lab (ONERA), Palaiseau, France, where he is currently principal scientist and member of the Scientific Committee of the ONERA Physics Branch. In January 2008, he joined the French-Singaporean SONDRA Lab on a part time basis to supervise Signal Processing topics. His current activities of research are centered in the topic of statistical signal processing for radar and SAR applications such as time-frequency, imaging, detection and parameters estimation.

Frédéric Pascal (M'08) was born in Sallanches, France in 1979. He received the Master's degree ("Probabilities, Statistics and Applications: Signal, Image et Networks") with merit, in applied statistics from University Paris VII–Jussieu, Paris, France, in 2003. He received the Ph.D. degree in signal processing, from University Paris X–Nanterre in 2006. This Ph.D. thesis was in collaboration with the French Aerospace Lab (ONERA), Palaiseau, France.

From November 2006 to February 2008, he held a post doctoral position in the Signal Processing and Information team of the Laboratory SATIE (Système et Applications des Technologies de l'Information et de l'Energie), CNRS, Ecole Normale Supérieure, Cachan, France. Since March 2008, he is an assistant professor in the SONDRA Laboratory, SUPELEC. His research interests are estimation in statistical signal processing and radar detection.